

Synthesis of ceria-based ceramics by combustion technique

C. MATEI, D. BERGER*, S. STOLERIU, D. NEAGU, E. STEFAN

University "Politehnica" of Bucharest, Faculty of Applied Chemistry and Material Science, 1-7 Polizu street, Bucharest, 011061, Romania

$Ce_{1-x}Gd_x/Sm_xO_{2-\delta}$ ($x=0.1, 0.2$) powders were prepared by combustion method using corresponding metallic nitrates and different fuels (α -alanine, oxamic hydrazide and tartaric acid). $Ce_{1-x}Gd_x/Sm_xO_{2-\delta}$ powders were formed direct from combustion reaction in one single step when oxamic hydrazide or α -alanine is used as fuel. In the case of tartarate-based precursors, the fluorite phase has been formed by calcining the as-prepared powders (the powders resulted in the combustion reaction) at 500 °C, 3h. The structure and thermal decomposition of the precursors, isolated before the ignition of the reaction mixture, were studied by FTIR spectroscopy and thermal analysis (DTA-TG). The oxide powders were investigated by X-ray diffraction and scanning electron microscopy. Densification of $Ce_{1-x}Gd_x/Sm_xO_{2-\delta}$ ($x=0.1, 0.2$) ceramic bodies was studied function of the doping ion and sintering conditions.

(Received April 22, 2010; accepted July 14, 2010)

Keywords: Combustion method, Solid oxide fuel cells, Ceria-based ceramics

1. Introduction

Solid oxide fuel cells (SOFCs) offer an efficient means to convert chemical energy to electricity by using a large variety of fuels, with potential applications in transportation, remote power, defence, etc. Up to now, many ceramic materials have been used as electrolyte in order to improve the reliability and to lower the operating temperature of the SOFCs. Among these, Gd/Sm doped ceria have showed promising results as solid electrolyte for intermediate temperature solid oxide fuel cells (IT-SOFCs) [1,2].

Among the wet chemical routes, the solution combustion technique offers a rapid synthesis procedure for very fine ceria-based nanopowders. The process is based on the redox reaction between Ce(III) and Gd(III) or Sm(III) nitrates and an organic compound that acts as fuel. The correct chosen of the fuel that is also a chelating agent is the key-factor for the success of this method and since now, ceria-based powders have been successfully synthesised by this method using glycine [3], urea [4], and citric acid [5,6] as fuel.

In this paper we present our results on the synthesis of $Ce_{1-x}Gd_x(Sm_x)O_{2-\delta}$ ($x=0.1, 0.2$) nanopowders obtained by solution combustion using different fuels, α -alanine, oxamic hydrazide and tartaric acid, correlated with the sintering conditions in order to obtain dense ceramics that can be used as electrolyte for IT-SOFC.

2. Experimental

Corresponding amounts of $Ce(NO)_3$ and $Gd(NO)_3$ or $Sm(NO)_3$ were dissolved in distilled water, to which α -

alanine ($CH_3-CH(NH_2)-COOH$, Ala), oxamic hydrazide, ($NH_2COCONHNH_2$, SOH) or tartaric acid ($HOOC-CH(OH)-CH(OH)-COOH$, TA) were added in stoichiometric amount ($\varphi=1$) or in 20% excess ($\varphi=1.2$). The molar ratio between metal nitrates and organic compound was calculated according to the rule of propellants. The reaction mixture was heated on a hot plate under magnetic stirring until ignited, burned and the as-prepared powder was formed.

The precursors were isolated before the combustion of the reaction mixture and dried in vacuum. The powders obtained directly from the combustion process, named as-prepared powders, were calcined at 500 °C, 3h to burn any residual carbon. The structure and thermal behaviour of isolated precursors were analysed by FT-IR spectra performed on Bruker Tensor 27 and thermal analysis, DTA-TG (Shimadzu TA60), respectively. The oxide powders were studied by X-ray diffraction (XRD) performed on a Rigaku Miniflex II diffractometer with $CuK\alpha$ radiation at 0.01°/s step. The crystallite sizes (D) were calculated by using Rigaku PDXL software. After grinding, the powders were pressed in pellets and sintered at 1300 ° or 1400 °C, 4h to obtain dense ceramic bodies that were investigated by XRD, SEM (Hitachi S 2600N microscope) and relative density measurements in ethanol (Archimede method).

3. Results and discussion

Precursors characterisation. The precursors isolated before the combustion reaction were analysed by FT-IR spectra and thermal analysis (DTA-TG).

DTA-TG analyses show violent decomposition at 206 °C of the alanine-based precursors and 262 °C of the oxamic hydrazide-based precursor, respectively (Fig. 1). The dopant nature and content have no significant contribution to the combustion reaction. The DTA curve of TA-based precursors (Fig. 1C) present an important exothermic effect around 130°C corresponding to the combustion of the reaction mixture ($\varphi=1$; 1.2) and a smaller one at 290 °C in the case of the precursor corresponding to $\varphi=1.2$ assigned to the burning of the excess of tartaric acid.

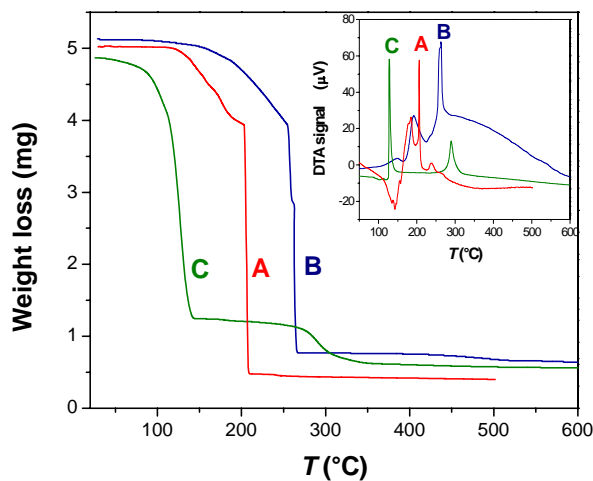


Fig. 1. TG curves of the alanine-based precursor (A); SOH-based precursor (B) and TA-based precursor, $\varphi = 1.2$ (C) of $Ce_{0.9}Gd_{0.1}O_{1.95}$ (inset, the corresponding DTA curves of the same precursors).

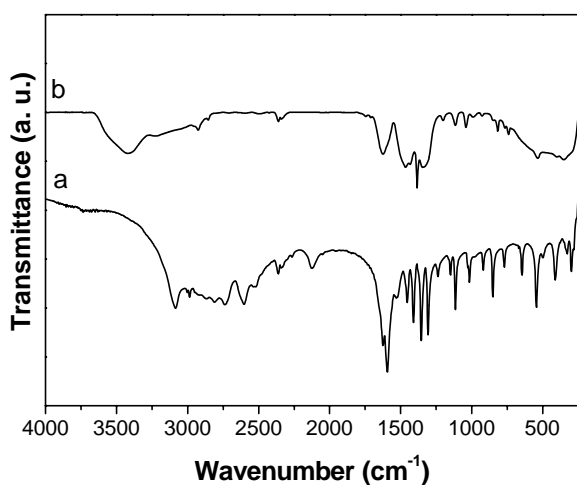


Fig. 2. FTIR spectra of α -alanine (a) and $Ce_{0.9}Gd_{0.1}O_{1.95}$ alanine-based precursor (b)

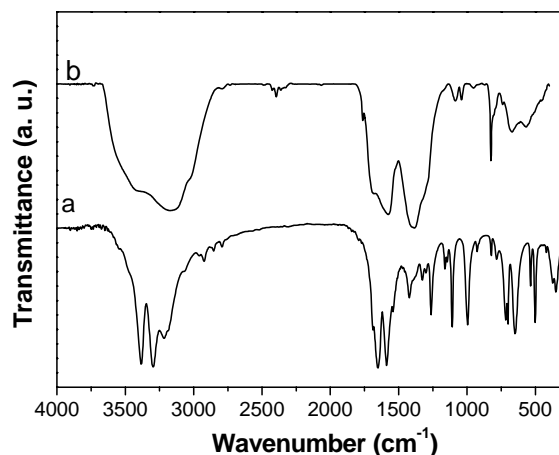


Fig. 3. FT-IR Spectra of oxamic hydrazide (a) and $Ce_{0.9}Gd_{0.1}O_{1.9}$ SOH-based precursor (b)

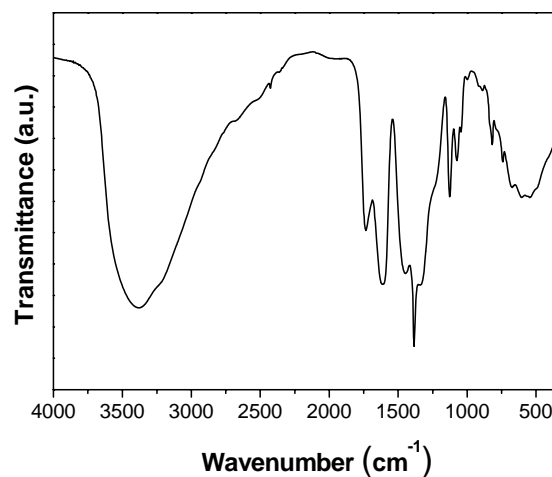


Fig. 4. FTIR spectrum of $Ce_{0.8}Gd_{0.2}O_{1.90}$ TA-based precursor ($\varphi = 1$)

All three fuels are also chelating agents and form complex compounds as FT-IR spectra have proved (Fig. 2-4). The coordination of α -alanine molecules by oxygen atom of CO group to lanthanoid cations is sustained by the presence in the FTIR spectrum of alanine-based precursor (Fig. 2b) of the shifted intense band from 1597 cm^{-1} ($\nu_{as}(CO)$ of alanine) to 1630 cm^{-1} . The coordination of alanine molecules to metal cations by nitrogen is proved by the shift of $\rho_r(NH_2)$ vibration mode from 1237 cm^{-1} (in the alanine spectrum (Fig. 2a)) to 1200 cm^{-1} in the precursor spectrum (Fig. 2b). [7] In the FTIR spectrum of SOH-based precursor it can be noticed the characteristic vibrations of NO_3^- ions (1385 cm^{-1} , 825 cm^{-1} , 1041 cm^{-1} and 741 cm^{-1} [7]), the shifted bands of the two carbonyl groups of SOH towards higher frequency values (ν_{CO} amide and hydrazide) from 1653 cm^{-1} and 1589 cm^{-1} to

1686 cm^{-1} and 1609 cm^{-1} , respectively, that can be assigned to the coordination of these groups to lanthanoid metal cations. The characteristic vibration of hydrazide group is present at 1159 cm^{-1} . The coordination of amine group of SOH molecule is sustained by the shifted vibrations, ρ_{NH_2} and δ_{NH_2} , from 1109 cm^{-1} and 700 cm^{-1} at 1088 cm^{-1} and 957 cm^{-1} , respectively (Fig. 3). [8] In the FTIR spectra of TA-based precursors (Fig. 4) it can be observed the presence of the shifted stretching vibrations of CO group towards lower frequency values (1618 cm^{-1} and 1454 cm^{-1}), as well as the OH group vibrations shifted from 3410 cm^{-1} and 3320 cm^{-1} at 3395 cm^{-1} and 3254 cm^{-1} , respectively, that sustained the formation of chelate-type compounds. In the FTIR spectra of TA-based precursor there is also present the vibration mode of tartaric acid nondeprotonated carboxyl group at 1738 cm^{-1} . [9]

Powders characterisation. Nanocrystalline $\text{Ce}_{1-x}\text{Gd}_x(\text{Sm}_x)\text{O}_{2-\delta}$ ($x=0.1, 0.2$) powders with fluorite structure and cubic symmetry were obtained directly from the combustion reaction, in a single step, as XRD data have proved when oxamic hydrazide or α -alanine were used as fuel (Figs. 5 and 6). In the case of tartarate-based systems, XRD data (Fig. 7) confirm the fluorite structure formation with cubic symmetry for all the samples annealed at 500 $^\circ\text{C}$, 3h. At combustion ratio ($\varphi=1$), the as-prepared powder has already the fluorite structure, but also some residual carbon (Fig. 7).

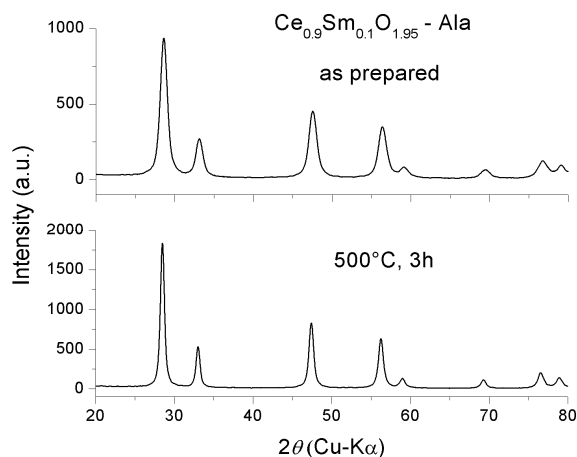


Fig. 5. XRD data of $\text{Ce}_{0.9}\text{Sm}_{0.1}\text{O}_{1.95}$ samples prepared from alanine-based precursors.

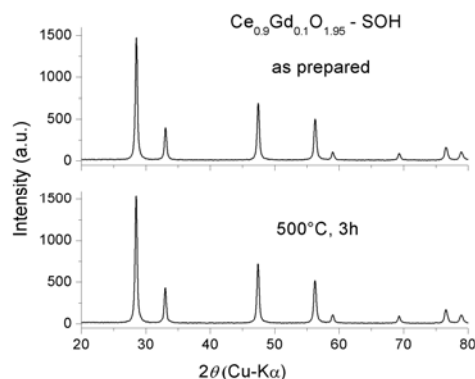


Fig. 6 XRD patterns of $\text{Ce}_{0.9}\text{Gd}_{0.1}\text{O}_{1.95}$ powders obtained from SOH-based precursors

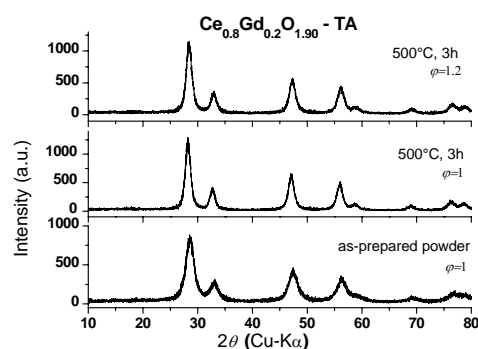


Fig. 7. XRD patterns of $\text{Ce}_{0.8}\text{Gd}_{0.2}\text{O}_{2.0}$ powders obtained from tartarate-based precursor

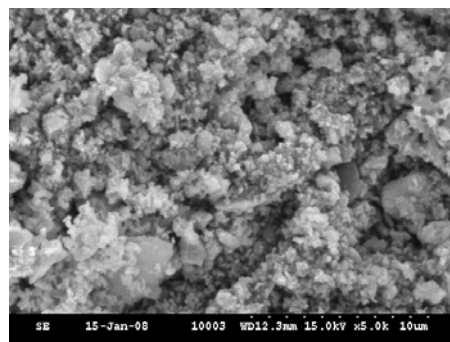


Fig. 8. SEM micrograph of $\text{Ce}_{0.9}\text{Sm}_{0.1}\text{O}_{1.95}$ powders obtained from tartarate-based precursor at 500 $^\circ\text{C}$

Table 1. Lattice parameters and crystallite size values for $Ce_{1-x}Gd_x(Sm_x)O_{2-\delta}$

Compound	Fuel	Thermal treatment	Lattice parameters		D (nm)
			a (Å)	V (Å ³)	
$Ce_{0.9}Sm_{0.1}O_{1.95}$	Ala ($\phi=1.2$)	as prepared	5.419	159.13	8
$Ce_{0.9}Sm_{0.1}O_{1.95}$	Ala ($\phi=1.2$)	500°C, 3h	5.424	159.57	14
$Ce_{0.9}Gd_{0.1}O_{1.95}$	Ala ($\phi=1.2$)	500°C, 3h	5.423	159.48	13
$Ce_{0.8}Gd_{0.2}O_{1.90}$	Ala ($\phi=1.2$)	as-prepared	5.437	160.72	15
$Ce_{0.8}Gd_{0.2}O_{1.90}$	Ala ($\phi=1.2$)	500°C, 3h	5.430	160.10	21
$Ce_{0.9}Sm_{0.1}O_{1.95}$	SOH ($\phi=1.2$)	as-prepared	5.417	158.96	27
$Ce_{0.8}Sm_{0.2}O_{1.90}$	SOH ($\phi=1.2$)	as-prepared	5.435	160.55	28
$Ce_{0.9}Gd_{0.1}O_{1.95}$	SOH ($\phi=1.2$)	as-prepared	5.422	159.36	23
$Ce_{0.9}Gd_{0.1}O_{1.95}$	SOH ($\phi=1.2$)	500°C, 3h	5.418	159.04	23
$Ce_{0.8}Gd_{0.2}O_{1.90}$	SOH ($\phi=1.2$)	as-prepared	5.418	159.03	32
$Ce_{0.9}Gd_{0.1}O_{1.95}$	TA ($\phi=1.0$)	500°C, 3h	5.423	159.48	7
$Ce_{0.9}Gd_{0.1}O_{1.95}$	TA ($\phi=1.2$)	500°C, 3h	5.424	159.57	7
$Ce_{0.9}Sm_{0.1}O_{1.95}$	TA ($\phi=1.2$)	500°C, 3h	5.406	157.99	7
$Ce_{0.9}Gd_{0.2}O_{1.90}$	TA ($\phi=1.0$)	500°C, 3h	5.326	151.08	6
$Ce_{0.9}Gd_{0.2}O_{1.90}$	TA ($\phi=1.2$)	500°C, 3h	5.435	160.54	6

The crystallite size values are different depending on the fuel; the powders obtained from tartarate-based precursors have the smallest values (Table 1). The sample morphology depends on the fuel used. The ceria-based samples obtained by TA-nitrate synthesis present fine primary particles with the tendency of spherical agglomerates formation of 1-2 μm diameter (Fig. 8) as SEM analysis has revealed. In the case of SOH method,

the agglomeration degree of the as prepared samples is lower than for the calcined powders (Fig. 9 a and b); the powders obtained from alanine-based precursors consist of agglomerates with irregular shapes and high porosity (Fig. 10c and d), whilst the oxide nanopowders obtained from SOH-based precursors present aggregates with sharp edges.

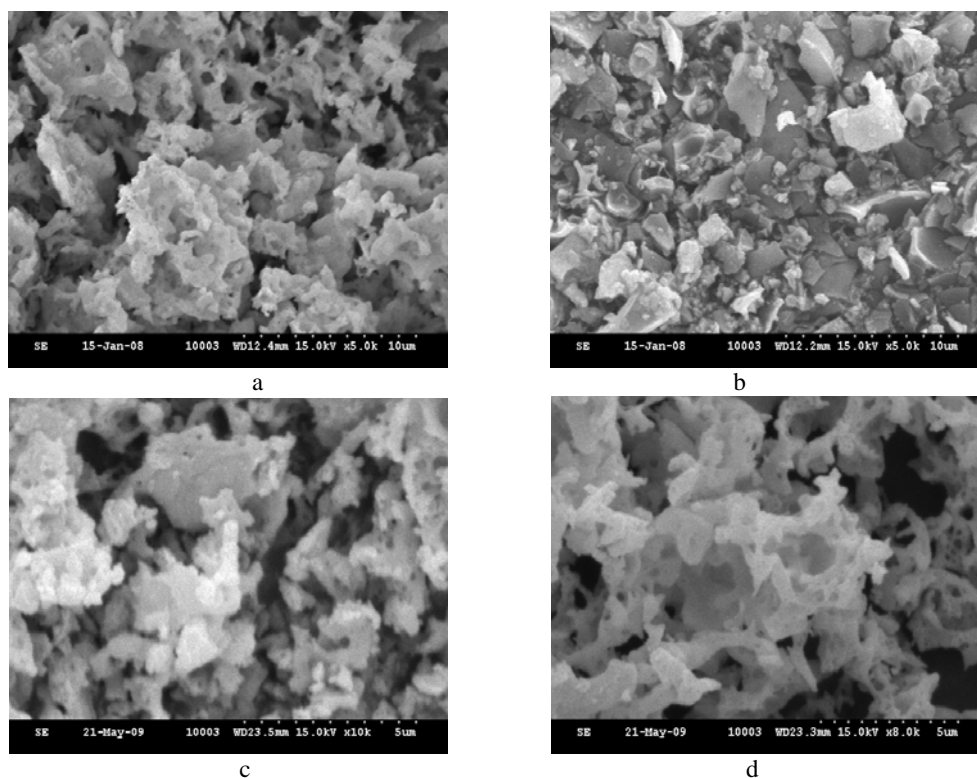


Fig. 9. SEM images of ceria-based nanopowders: (a) $Ce_{0.9}Gd_{0.1}O_{1.95}$ as-prepared powder obtained from SOH-based precursor; (b) $Ce_{0.9}Gd_{0.1}O_{1.95}$ obtained at 500 °C by SOH-nitrate synthesis; (c) $Ce_{0.8}Gd_{0.2}O_{1.90}$ as-prepared powder obtained by alanine - nitrate method; (d) $Ce_{0.8}Gd_{0.3}O_{1.90}$ obtained at 500 °C by alanine - nitrate method;

Ceramic samples characterisation. Samples sintered at 1300 °C, 4h have relative density values in the range of 80-90%, whereas a thermal treatment at 1400 °C, 4h increase the relative density up to 99% (Table 2). Ceramic bodies sintered at 1400 °C, 4h present different microstructures (Figs. 10 and 11) depending on the fuel used in the synthesis and the doping ion nature and content.

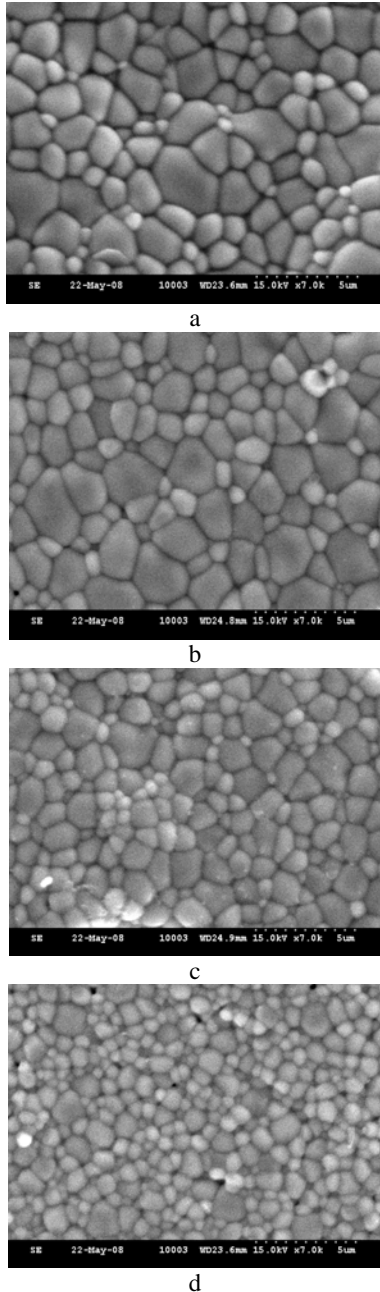
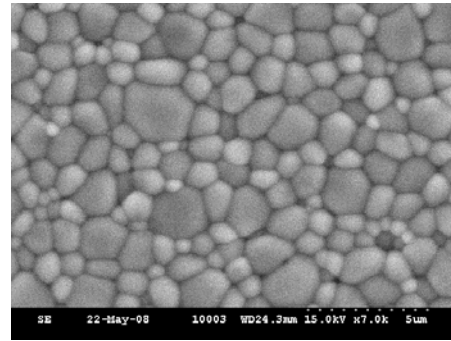
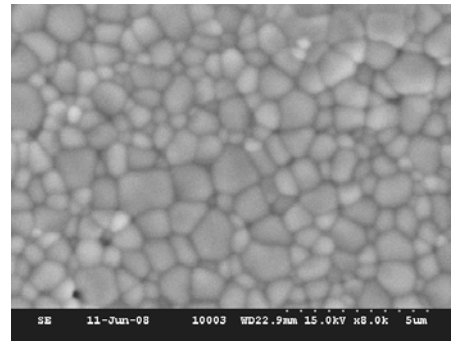


Fig. 10. SEM images of ceramics samples sintered at 1400°C, 4h: (a) $Ce_{0.9}Gd_{0.1}O_{1.95}$ obtained from alanine-based precursor; (b) $Ce_{0.9}Gd_{0.1}O_{1.95}$ obtained from SOH-based precursor; $Ce_{0.9}Sm_{0.1}O_{1.95}$ samples obtained from: (c) Ala-precursor; (d) SOH-precursor.



a



b

Fig. 11. SEM micrographs of the ceramic samples sintered at 1400°C, 4h, obtained by nitrate-tartarate synthesis: (a) $Ce_{0.9}Gd_{0.1}O_{1.95}$; (b) $Ce_{0.8}Gd_{0.2}O_{1.90}$

The smaller grains were observed for Sm-doped samples, especially in the case of SOH method (around 1µm) than for the grains of Gd-doped ceramic samples. The increase of doping ion content, especially in the case of gadolinium, leads to the formation of some intergranular pores. These observations based on the SEM investigation are in good agreement with the relative density values measured by Archimede method in ethanol. Table 2 lists the density values of the ceramic bodies sintered at 1400 °C, 4h obtained from powders presented in this paper.

Table 2. Density values of $Ce_{1-x}Gd_x(Sm_x)O_{2-\delta}$ ceramics sintered at 1400°C, 4h

Sample	Fuel	Density (g/cm^3)	d (%)
$Ce_{0.9}Sm_{0.1}O_{1.95}$	Ala ($\varphi=1.2$)	6.64	91.9
$Ce_{0.9}Gd_{0.1}O_{1.95}$	Ala ($\varphi=1.2$)	6.72	93.0
$Ce_{0.8}Gd_{0.2}O_{1.90}$	Ala ($\varphi=1.2$)	6.45	89.0
$Ce_{0.9}Sm_{0.1}O_{1.95}$	SOH ($\varphi=1.2$)	6.79	93.9
$Ce_{0.8}Sm_{0.2}O_{1.90}$	SOH ($\varphi=1.2$)	6.54	91.5
$Ce_{0.9}Gd_{0.1}O_{1.95}$	SOH ($\varphi=1.2$)	6.93	96.6
$Ce_{0.8}Gd_{0.2}O_{1.90}$	SOH ($\varphi=1.2$)	6.28	86.2
$Ce_{0.9}Gd_{0.1}O_{1.95}$	TA ($\varphi=1.2$)	6.72	93.61
$Ce_{0.9}Sm_{0.1}O_{1.95}$	TA ($\varphi=1.2$)	7.24	99.00
$Ce_{0.9}Gd_{0.1}O_{1.95}$	TA ($\varphi=1.0$)	6.80	94.0
$Ce_{0.8}Gd_{0.2}O_{1.90}$	TA ($\varphi=1.0$)	6.67	92.1

4. Conclusions

The combustion technique is suitable to prepare ceria-based nanopowders. Well-sintered ceramic bodies have been obtained at relative low temperature by this method. The sintering ability of ceria-based ceramics depends on the dopant content and type, as well as the fuel used in the synthesis. Gd-doped samples present higher relative density values compared to Sm-doped samples for $x=0.1$ and the opposite for $x=0.2$ in the case of alanine- nitrate and oxamic hydrazide-nitrate syntheses. The ceramic bodies obtained from tartarate-based systems have higher density values than the ceramics prepared by the other two methods. It has been noticed that the relative density values decrease with the dopant content, for both dopants, but significantly for Gd-doped ceramics.

Acknowledgements

This research has been supported by the Romanian project PNCDI no. 71-030/2007.

References

- [1] J. M. Ralph, A.C. Schoeler, M. Krumpelt, J. Mater. Sci. **36**, 1161 (2001).
- [2] S. Hui, J. Roller, S. Yick, X. Zhang, C. Decès-Petit, Y. Xie, R. Maric, D. Ghosh, J. Power Sources **172**, 493 (2007).
- [3] K. Singh, S.A. Acharya, S.S. Bhoga, Ionics **12**, 295 (2006).
- [4] E. Chinarro, J.R. Jurado, M.T. Colomer, J. Eur. Ceram. Soc. **27**, 3619 (2007).
- [5] H. M. Xu, H. G. Yan, Z. H. Chen, Mater. Charact. **59**, 301 (2008).
- [6] T. Mahata, G. Das, R.K. Mishra, B.P. Sharma, J. Alloy. Compd. **391**, 129 (2005).
- [7] K. Nakamoto, Infrared and Raman spectra of inorganic and coordination compounds, Part B, John Wiley and Sons, New York, 1997.
- [8] G. N. R. Tripathi, J. E. Katon, J. Molec. Structure **54**, 19 (1979).
- [9] S. A. Martin Britto Dhas, M. Suresh, G. Bhagavannarayana, S. Natarajan, J. Crystal Groth **309**, 48 (2007).

*Corresponding author: danaberger01@yahoo.com